Northwell Health℠

HOFSTRA NORTHWELL SCHOOL of MEDICINE AT HOFSTRA UNIVERSITY

Journal Articles

Donald and Barbara Zucker School of Medicine Academic Works

2015

New best1 mutations in autosomal recessive bestrophinopathy

A. T. Fung

S. Yzer

N. Goldberg

H. Wang

M. Nissen

See next page for additional authors

Follow this and additional works at: https://academicworks.medicine.hofstra.edu/articles


Part of the Ophthalmology Commons

Recommended Citation

Fung A, Yzer S, Goldberg N, Wang H, Nissen M, Giovannini A, Merriam J, Bukanova E, Yannuzzi LA, Allikmets R, . New best1 mutations in autosomal recessive bestrophinopathy. . 2015 Jan 01; 35(4):Article 1707 [p.]. Available from: https://academicworks.medicine.hofstra.edu/articles/1707. Free full text article.

This Article is brought to you for free and open access by Donald and Barbara Zucker School of Medicine Academic Works. It has been accepted for inclusion in Journal Articles by an authorized administrator of Donald and Barbara Zucker School of Medicine Academic Works.

Authors
A. T. Fung, S. Yzer, N. Goldberg, H. Wang, M. Nissen, A. Giovannini, J. E. Merriam, E. N. Bukanova, L. A. Yannuzzi, R. Allikmets, and +2 additional authors

This article is available at Donald and Barbara Zucker School of Medicine Academic Works:
https://academicworks.medicine.hofstra.edu/articles/1707

Author Manuscript

Author Manuscript

Author Manuscript

Author Manuscript

HHS Public Access

Author manuscript

Retina. Author manuscript; available in PMC 2015 May 09.

Published in final edited form as:

Retina. 2015 April ; 35(4): 773–782. doi:10.1097/IAE.0000000000000387.

NEW *BEST1* MUTATIONS IN AUTOSOMAL RECESSIVE BESTROPHINOPATHY

ADRIAN T. FUNG, MMed[*,‡‡,§§], **SUZANNE YZER, MD, PhD**[*,†], **NAOMI GOLDBERG, MD**[*,‡], **HAO WANG, MD**[¶], **MICHAEL NISSEN, MD**[**], **ALFONSO GIOVANNINI, MD**[††], **JOANNA E. MERRIAM, MD, PhD**[†], **ELENA N. BUKANOVA, MD**[†], **CAROLYN CAI, BA**[†], **LAWRENCE A. YANNUZZI, MD**[*,†], **STEPHEN H. TSANG, MD, PhD**[†,§], and **RANDO ALLIKMETS, PhD**[†,§]

[*]Vitreous-Retina-Macula Consultants of New York and the LuEsther T. Mertz Retinal Research Center, Manhattan Eye, Ear, and Throat Institute, New York, New York

[†]Department of Ophthalmology, Columbia University, New York, New York

[‡]Department of Ophthalmology, Icahn School of Medicine at Mount Sinai, New York, New York

[§]Department of Pathology and Cell Biology, Columbia University, New York, New York

[¶]Albany Medical Center, Albany, New York

[**]Department of Ophthalmology, Weill Cornell Medical College, New York, New York

[††]Ophthalmology Section, Department of Neuroscience, Polytechnic University of Marche, Ancona, Italy

[‡‡]Australian School of Advanced Medicine, Macquarie University Hospital, Sydney, Australia

[§§]Save Sight Institute, University of Sydney, Sydney, Australia

Abstract

Purpose—To report the ocular phenotype in patients with autosomal recessive bestrophinopathy and carriers, and to describe novel *BEST1* mutations.

Methods—Patients with clinically suspected and subsequently genetically proven autosomal recessive bestrophinopathy underwent full ophthalmic examination and investigation with fundus autofluorescence imaging, spectral domain optical coherence tomography, electroretinography, and electrooculography. Mutation analysis of the *BEST1* gene was performed through direct Sanger sequencing.

Results—Five affected patients from four families were identified. Mean age was 16 years (range, 6–42 years). All affected patients presented with reduced visual acuity and bilateral, hyperautofluorescent subretinal yellowish deposits within the posterior pole. Spectral domain optical coherence tomography demonstrated submacular fluid and subretinal vitelliform material

Copyright © by Ophthalmic Communications Society, Inc. Unauthorized reproduction of this article is prohibited.

Reprint requests: Rando Allikmets, PhD, Eye Institute Research, Room 202, 160 Fort Washington Avenue, New York, NY 10032; rla22@columbia.edu.

A. T. Fung and S. Yzer are co-first authors.

None of the authors have any financial/conflicting interests to disclose.

Author Manuscript Author Manuscript Author Manuscript Author Manuscript

in all patients. A cystoid maculopathy was seen in all but one patient. In 1 patient, the location of the vitelliform material was seen to change over a follow-up period of 3 years despite relatively stable vision. Visual acuity and fundus changes were unresponsive to topical and systemic carbonic anhydrase inhibitors and systemic steroids. Carriers had normal ocular examinations including normal fundus autofluorescence. Three novel mutations were detected.

Conclusion—Three novel *BEST1* mutations are described, suggesting that many deleterious variants in *BEST1* resulting in haploinsufficiency are still unknown. Mutations causing autosomal recessive bestrophinopathy are mostly located outside of the exons that usually harbor vitelliform macular dystrophy–associated dominant mutations.

Keywords

autosomal recessive bestrophinopathy; *BEST1* gene; deleterious mutations; vitelliform

BEST1 (VMD2) is a gene located on the long arm of chromosome 11 (*11q12.3*) that encodes for the 585 amino acid transmembrane protein bestrophin 1, located on the basolateral aspect of retinal pigment epithelial (RPE) cells.[1] The exact function of bestrophin 1 is still not unequivocally characterized, but it is linked to transepithelial chloride flow possibly by controlling Ca^{2+} channels in the RPE.[1–3] Mutations in *BEST1* therefore affect RPE metabolism, and by consequence outer retinal function with which the RPE is intimately associated. Over 200 mutations in *BEST1* have been identified and published.[1,3,4] Mutations are associated with Best vitelliform macular dystrophy (VMD, MIM 153700), adult-onset vitelliform macular dystrophy (MIM 608161), retinitis pigmentosa 50 (RP50, MIM 613194), and autosomal dominant vitreoretinochoroidopathy (MIM 193220). These diseases are all caused by autosomal dominant mutations. Recently, a phenotype caused by autosomal recessive mutations in *BEST1* was described: autosomal recessive bestrophinopathy (ARB, OMIM 611809).

Autosomal recessive bestrophinopathy is a rare ocular disease. It was defined by Burgess et al[1] in 2008, although the same condition with compound heterozygous mutations in *VMD2* had been described 2 years earlier.[5] It results from biallelic mutations in *BEST1* and is characterized by a multifocal vitelliform dystrophy with subretinal fluid. An association with hypermetropia and angle closure has been described.[1] Herein, we review the clinical features and mutation analysis of four families with ARB.

Materials and Methods

Patients and Clinical Analyses

All patients underwent a complete ophthalmic examination by a retinal physician. This included best-corrected visual acuity, cycloplegic refraction, slit-lamp biomicroscopy, and dilated funduscopy. All patients underwent color fundus photography, fundus autofluorescence imaging, and spectral domain optical coherence tomography. In addition, Patient 4 underwent fluorescein and indocyanine green angiography. When possible, patients had electroretinography and electrooculography performed under the International Society for Clinical Electrophysiology of Vision standards.[6,7] Peripheral blood was drawn for genetic testing. Patients provided written informed consent for all procedures, which

Author Manuscript Author Manuscript Author Manuscript Author Manuscript

were approved by the Ethics Committees of the sites involved and adhered to the Declaration of Helskinki (Institutional Review Board protocol #AAAB6560 Columbia University).

Genetic Analyses

All 11 exons of *BEST1* gene were sequenced by Sanger direct sequencing method to obtain sequences for all coding sequences, the noncoding Exon 1, and 50bp of adjacent intronic sequences of each exon. Primer sequences are available on request. Messenger RNA was isolated from venous blood using QIAamp RNA Blood Mini Kit (QIAGEN Cat. No. 75142) with a fast spin-column procedure. Genomic DNA is eliminated by pre-treating the RNA sample with DNase I, Amplification Grade (Invitrogen Cat. No. 18068-015 DNase I Amplification Grade; Invitrogen, Carlsbad, CA). The primer pair was designed to encompass *BEST1* Exons 1 and 2. Forward primer was in the Exon 1 of BEST1, 5′ACCAGCCTAGTCGCCAGA3′ (1) and the reverse primer in the Exon 2 of *BEST1*, 5′GCGGATGATGTAGTAGCAGAG3′ (2). The final concentration for each primer was 0.2 μmol. The thermal cycling conditions were established using a ABI 9700 thermocycler (Applied Biosystems, Foster City, CA). Efficient complementary DNA synthesis was achieved in a 30-minute incubation at 55° C. Polymerase chain reaction (PCR) amplification consisted of 40 cycles of 94°C for 15 seconds, 65° C for 30 seconds, and 68°C for 1 minute. We used 1 cycle 68°C for 5 minutes for final extension.

Results

Five patients from four families with genetically confirmed ARB were identified. Mean age was 16 years (range, 6–42 years). Two patients (Patients 3 and 5) were the product of a consanguineous marriage. All patients presented with reduced visual acuity and bilateral, subretinal yellowish deposits within the posterior pole that showed increased autofluorescence on fundus autofluorescence imaging. On spectral domain optical coherence tomography, submacular fluid and subretinal changes suggestive of vitelliform material were present in all patients. In 1 patient (Patient 4), the location of the vitelliform material was seen to change over a follow-up period of 3 years with relatively stable vision. A cystoid maculopathy was seen in all but one patient (Patient 5). Visual acuity and fundus changes were unresponsive to topical and systemic carbonic anhydrase inhibitors and systemic steroids. Both parents of Patient 3 had normal ocular examinations including normal 20/20 vision, normal fundus autofluorescence, and a completely normal spectral domain optical coherence tomography. Clinical features and investigations are described below and summarized in Figures 1–4 and Tables 1–3.

Family 1, Patients 1 and 2

A 11-year-old otherwise healthy white boy presented with a 6-month history of reduced vision and central scotoma (Figure 1). His vision was 20/25 in both eyes, and there was no evidence of angle closure. Bilateral, multifocal subretinal hyperautofluorescent yellowish deposits extended from the posterior poles up to the equator. Cystoid macular edema and shallow serous macular detachments were present in both eyes. Treatment with topical nepafenac 0.1% (1 month) and prednisone 10 mg PO (3 weeks) failed to improve vision or

Author Manuscript Author Manuscript Author Manuscript Author Manuscript

the fundus appearance. His 7-year-old brother was subsequently found to have almost identical clinical findings, whereas his 9-year-old sister and parents were unaffected.

Compound heterozygous BEST1 variants were identified in the affected patients. The first was a novel c.728C>A; p.Ala243Glu missense mutation in Exon 7. In the same codon, previously reported *BEST1* variants include p.Ala243Val[8] and p.Ala243Thr.[9] Both the nucleotide and the amino acid are highly conserved in this position of *BEST1*. All predictive programs suggest that the variant is disease-causing or disease-damaging. Therefore, it is highly likely that this variant is deleterious as are (almost) all *BEST1* variants implicated in ARB. The second mutation, the previously described c.598C>T; p.Arg200* mutation,[1] generates a stop codon and results in a truncated protein at position 200.

Family 2, Patient 3

A 6-year-old asymptomatic, U.S.–born African boy was noted to have poor vision by his schoolteacher (Figure 2). A history of consanguinity was present in the family, with his parents being first cousins. Bilateral, multifocal curvilinear subretinal hyperautofluorescent yellowish deposits were present in both eyes with cystic edema and subretinal fluid at the maculae. Subfoveal choroidal thicknesses were 586 μm in the right eye and 482 mm in the left eye. Trials of topical dorzolamide 2% 3 times a day in both eyes (6 weeks), acetazolamide 500 mg nocte (2 months), and prednisone failed to improve vision or the clinical appearance. Three years after first presentation, the vision remained stable at 20/80 in both eyes. All other family members were clinically unaffected.

A novel, homozygous deleterious mutation was identified in the proband in the in-frame deletion of 3 nucleotides, c.847_849delTTC, which results in a homozygous deletion of phenylalanine at position 283, p.Phe283del.

Family 3, Patient 4

A 12-year-old otherwise healthy, emmetropic Puerto Rico–born U.S. boy was noted to have reduced vision on routine eye examination. Bilateral, confluent curvilinear subretinal hyperautofluorescent yellowish vitelliform deposits became more multifocal and dispersed over 3 years of follow-up (Figure 3). Bilateral multifocal serous retinal detachments and cystic edema involved both maculae. Subfoveal choroidal thickness was 537 μm in the right eye and 527 μm in the left eye. Oral prednisone 60 mg daily (3 months), topical dorzolamide 2% 3 times a day in both eyes (6 weeks), and oral acetazolamide (6 weeks) were trialed to reduce the cystoid maculopathy with no clinical response.

A previously described[10] homozygous c.821C>G; p.Pro274Arg variant was detected. This variant of a highly conserved nucleotide and an amino acid is predicted to be deleterious by all predictive programs.

Family 4, Patient 5

A 42-year-old woman whose vision problems started at 5 years of age was recently noticing deteriorating central vision (Figure 4). She was the product of a first-cousin marriage. A white-yellow vitelliform lesion was present at the left fovea, and RPE and retinal atrophy

Author Manuscript Author Manuscript Author Manuscript Author Manuscript

within the posterior poles. Shallow subretinal but not intraretinal fluid was present at both maculae. Subfoveal choroidal thickness was 370 μm in both eyes. A trial of oral acetazolamide 500 mg failed to improve the vision.

A splice site variant, c.-29+5G>A (IVS1+5G>A), was identified in Intron 1 of *BEST1* in the donor site of the first untranslated exon. This exon is usually not screened for variants in patients with *BEST1*-associated diseases. As shown in Table 3, the variant practically abolishes the splice donor site as predicted by all programs. To confirm the functional consequences of this variant, we performed the splicing studies through an "illegitimate transcript" strategy. Although the *BEST1* gene is expressed only in the retinal pigment epithelium, it can also be detected by PCR at very low levels from other cells, such as the leucocytes in peripheral blood. We isolated messenger RNA from a blood sample of Patient 5 and performed PCR encompassing two exons. As seen in Figure 5, the messenger RNA of a normal control produced the expected PCR fragment in the situation where the splicing had been performed correctly. In this patient, homozygous for the IVS1+5G>A variant, the expected PCR product of 234bp was not detected and it was clear that the splicing of *BEST1* gene was incorrect, very likely resulting in no functional messenger RNA and, consequently, no *BEST1* protein.

Discussion

Autosomal recessive bestrophinopathy is a rare disease, with only a few case series described.[1,5,10,12–17] The timing of presentation is variable, with patients as young as 3 years[10] and as old as 45 years[13] being reported. Patients are typically hyperopic and present with moderately reduced vision, bilateral multifocal hyperautofluorescent vitelliform lesions with foveal involvement, and shallow retinal detachment. Scotopic and photopic full-field electroretinographies usually diminish with age, and the electrooculography shows a reduced or absent light rise (Arden ratio 1.0).

Our patients' phenotypes are all very consistent with these previous reports of ARB, although some interesting observations can be made. In one case (Patient 1), the vitelliform material appeared to emanate from the RPE on spectral domain optical coherence tomography. In 3 patients (Patients 1, 3, and 4), the retinal architecture was abnormal with thickening of Band 2 (traditionally described as the inner segment/outer segment junction), even in extramacular attached retina. Although it would be easy to ascribe this to vitelliform material, this area of "Band 2" thickening did not uniformly hyperautofluoresce and may instead represent elongation of degenerate photoreceptors. In four patients (Patients 1–4), the presence of a cystoid maculopathy was striking. This had been reported previously[10,12,13,16,17] and may represent perturbation of the blood–retinal barrier. Inflammation is less likely given the lack of anterior chamber or vitreous cells, optic neuritis, or vasculitis in all these patients. This cystic edema was absent in the eldest patient (Patient 5, 42 –years old). It is possible that with time, the multifocal vitelliform material in pediatric cases of ARB resolves. Subfoveal choroidal thickness was measured by enhanced depth imaging optical coherence tomography in three patients (Patients 3–5), with thickening in Patient 5. Unfortunately, not only has choroidal thickness not been described in ARB before, but normative data only apply to adults[19] and are lacking in the pediatric

Author Manuscript Author Manuscript Author Manuscript Author Manuscript

population. It is therefore difficult to determine if the choroidal thickness was pathologic in Patients 3 and 4.

Patient 4 had a 3-year follow-up and demonstrated dispersion and a change in location of the vitelliform material from superior to nasal to the optic disks. This is one of the longest follow-ups of a patient with ARB that we are aware of, and the first to describe fluctuation and dispersion in appearance. This patient also had indocyanine green angiography, which has only been described once before in ARB.[15] There was bilateral midphase hyperfluorescence at both maculae, which colocalized with the area of fluorescein leakage. This may represent leakage of indocyanine green dye into the shallow neurosensory detachments or choroidal hyperpermeability. Lipofuscin-rich vitelliform material does not normally stain with indocyanine green dye.[20] In VMD, which has similarities to ARB, small, peripheral hyperfluorescent spots on indocyanine green angiography have been described,[20] and histopathology has shown involvement not only of the retina and RPE but also of fibrillar material and electron-dense particles on electron microscopy within the choroid.[21,22]

Attempts at managing the cystic macular changes with topical and systemic carbonic anhydrase inhibitors and systemic steroids proved unsuccessful. However, it must be emphasized that the medications, dosages, and durations were not standardized, and Patient 2 was not prescribed any treatment.

We identified 3 novel *BEST1* mutations (c.728C>A [p.Ala243Glu] in Family 1, c. 847_849delTTC [p.Phe283-del] in Patient 3, and IVS1+5G>A in Patient 5), suggesting that many deleterious variants in *BEST1* resulting in loss of function are still unknown. It has been hypothesized that the ARB phenotype is caused by mutations that occur in the intracellular loop of the protein[10] or that the presence of two null alleles lead to disease. We agree that autosomal recessive mutations in *BEST1* that lead to ARB are most likely deleterious while autosomal dominant mutations in *BEST1* lead to VMD because of a dominant negative effect. Based on our results and reviewing those previously described, we also suggest that the dominant and recessive mutations mostly do not overlap and that the recessive mutations are located throughout the gene.

Other conditions can mimic the phenotypic appearance of ARB. These include multifocal Best disease, adult-onset VMD, multifocal pattern dystrophy associated with peripherin/*RDS* mutations, acute, exudative polymorphous vitelliform maculopathy, and paraneoplastic syndromes or metastases.[23–26] In addition, chronic, central serous choroidopathy can present with serous retinal detachments, cystoid maculopathy, and subretinal fibrin, although fibrin does not hyperautofluoresce. Boon et al[23] studied clinical and genetic heterogeneity in 15 patients with a multifocal vitelliform phenotype. Nine of these patients carried a *BEST1* mutation and one a peripherin/*RDS* mutation. Not only were the phenotypic appearance of patients with *BEST1* mutations diverse, but some of the patients without mutations in *BEST1* presented with a fundus appearance identical to the patients we describe in this study. Incorrect initial diagnoses in our patients included acute exudative polymorphous vitelliform maculopathy, Vogt–Koyanagi–Harada disease, and fundus flavimaculatus. Comprehensive

Author Manuscript Author Manuscript Author Manuscript Author Manuscript

screening by sequencing of the entire *BEST1* gene is therefore essential for the correct classification of these patients.

In summary, we report five patients from four families where affected individuals presented with ARB. Genetic analyses confirmed the disease in all families and showed segregation of likely deleterious, homozygous, or compound heterozygous mutations in *BEST1* with the disease phenotype. This study highlights several important points for the management of ARB:

1. Visual acuity remains relatively stable, although the fundus vitelliform pattern may fluctuate and diminish with time
2. Subretinal fluid and cystoid macular changes associated with ARB do not respond to topical and systemic carbonic anhydrase inhibitors or systemic steroids
3. Three of the five mutations were novel, suggesting that many deleterious variants in *BEST1* resulting in loss of function are still unknown
4. Sequencing of the entire gene is required to avoid missing any *BEST1* mutations. Mutations causing ARB are mostly located outside of the exons that usually harbor VMD-associated dominant mutations (Exons 2–6 of *BEST1*)
5. Mutations causing VMD and ARB rarely overlap. The former have a dominant negative effect causing disease phenotype in a heterozygous state. The latter delete the *BEST1* protein but do not cause the disease in heterozygosity, because carriers of recessive *BEST1* mutations (all parents and some siblings of ARB cases) have a normal phenotype
6. Because the phenotype of ARB may mimic other diseases, molecular genetic confirmation of mutations in *BEST1* is required to confirm the diagnosis.

Acknowledgments

Supported in part by the Macula Foundation, Inc by Stichting Wetenschappelijk Onderzoek Oogziekenhuis Rotterdam, Rotterdamse Blindenbelangen, Stichting Blindenhulp, Gelderse Blinden Stichting, Landelijke Stichting voor Blinden en Slechtzienden and grants from the National Eye Institute/NIH EY021163, EY019861, EY018213, EY019007 (Core Support for Vision Research), and unrestricted funds from Research to Prevent Blindness, New York, NY to the Department of Ophthalmology, Columbia University.

References

1. Burgess R, Millar ID, Leroy BP, et al. Biallelic mutation of BEST1 causes a distinct retinopathy in humans. Am J Hum Genet. 2008; 82:19–31. [PubMed: 18179881]
2. Johnson AA, Lee Y, Chadburn AJ, et al. Disease-causing mutations associated with four bestrophinopathies exhibit disparate effects on the localization, but not the oligomerization, of Bestrophin-1. Exp Eye Res. 2014; 121:74–85. [PubMed: 24560797]
3. Pasquay C, Wang LF, Lorenz B, Preising MN. Bestrophin 1— phenotypes and functional aspects in bestrophinopathies. Ophthalmic Genet. 2013:1–20.
4. Available at: http://www.retina-international.org/sci-news/databases/mutation-database/best1-mutation/http://www.retina-international.org/sci-news/databases/mutation-database/best1-mutation/
5. Schatz P, Klar J, Andreasson S, et al. Variant phenotype of Best vitelliform macular dystrophy associated with compound heterozygous mutations in VMD2. Ophthalmic Genet. 2006; 27:51–56. [PubMed: 16754206]

Author Manuscript Author Manuscript Author Manuscript Author Manuscript

6. Marmor MF, Fulton AB, Holder GE, et al. ISCEV standard for full-field clinical electroretinography (2008 update). Doc Ophthalmol. 2009; 118:69–77. [PubMed: 19030905]
7. Marmor MF, Brigell MG, McCulloch DL, et al. International Society for Clinical Electrophysiology of V. ISCEV standard for clinical electro-oculography (2010 update). Doc Ophthalmol. 2011; 122:1–7. [PubMed: 21298321]
8. Kramer F, White K, Pauleikhoff D, et al. Mutations in the VMD2 gene are associated with juvenile-onset vitelliform macular dystrophy (Best disease) and adult vitelliform macular dystrophy but not age-related macular degeneration. Eur J Hum Genet. 2000; 8:286–292. [PubMed: 10854112]
9. Lotery AJ, Munier FL, Fishman GA, et al. Allelic variation in the VMD2 gene in best disease and age-related macular degeneration. Invest Ophthalmol Vis Sci. 2000; 41:1291–1296. [PubMed: 10798642]
10. Kinnick TR, Mullins RF, Dev S, et al. Autosomal recessive vitelliform macular dystrophy in a large cohort of vitelliform macular dystrophy patients. Retina. 2011; 31:581–595. [PubMed: 21273940]
11. Kaplan J, Kahn A, Chelly J. Illegitimate transcription: its use in the study of inherited diseases. Hum Mutat. 1992; 1:357–360. [PubMed: 1301944]
12. Borman AD, Davidson AE, O'Sullivan J, et al. Childhood-onset autosomal recessive bestrophinopathy. Arch Ophthalmol. 2011; 129:1088–1093. [PubMed: 21825197]
13. Davidson AE, Sergouniotis PI, Burgess-Mullan R, et al. A synonymous codon variant in two patients with autosomal recessive bestrophinopathy alters in vitro splicing of BEST1. Mol Vis. 2010; 16:2916–2922. [PubMed: 21203346]
14. Gerth C, Zawadzki RJ, Werner JS, Heon E. Detailed analysis of retinal function and morphology in a patient with autosomal recessive bestrophinopathy (ARB). Doc Ophthalmol. 2009; 118:239–246. [PubMed: 18985398]
15. Guerriero S, Preising MN, Ciccolella N, et al. Autosomal recessive bestrophinopathy: new observations on the retinal phenotype—clinical and molecular report of an Italian family. Ophthalmologica. 2011; 225:228–235. [PubMed: 21412020]
16. Pineiro-Gallego T, Alvarez M, Pereiro I, et al. Clinical evaluation of two consanguineous families with homozygous mutations in BEST1. Mol Vis. 2011; 17:1607–1617. [PubMed: 21738390]
17. Zhao L, Grob S, Corey R, et al. A novel compound heterozygous mutation in the BEST1 gene causes autosomal recessive Best vitelliform macular dystrophy. Eye (Lond). 2012; 26:866–871. [PubMed: 22422030]
18. Spaide RF, Curcio CA. Anatomical correlates to the bands seen in the outer retina by optical coherence tomography: literature review and model. Retina. 2011; 31:1609–1619. [PubMed: 21844839]
19. Margolis R, Spaide RF. A pilot study of enhanced depth imaging optical coherence tomography of the choroid in normal eyes. Am J Ophthalmol. 2009; 147:811–815. [PubMed: 19232559]
20. Maruko I, Iida T, Spaide RF, Kishi S. Indocyanine green angiography abnormality of the periphery in vitelliform macular dystrophy. Am J Ophthalmol. 2006; 141:976–978. [PubMed: 16678528]
21. Weingeist TA, Kobrin JL, Watzke RC. Histopathology of Best's macular dystrophy. Arch Ophthalmol. 1982; 100:1108–1114. [PubMed: 7092654]
22. Frangieh GT, Green WR, Fine SL. A histopathologic study of Best's macular dystrophy. Arch Ophthalmol. 1982; 100:1115–1121. [PubMed: 7092655]
23. Boon CJF, Klevering BJ, den Hollander AI, et al. Clinical and genetic heterogeneity in multifocal vitelliform dystrophy. Arch Ophthalmol. 2007; 125:1100–1106. [PubMed: 17698758]
24. Grunwald L, Kligman BE, Shields CL. Acute exudative polymorphous paraneoplastic vitelliform maculopathy in a patient with carcinoma, not melanoma. Arch Ophthalmol. 2011; 129:1104–1106. [PubMed: 21825203]
25. Khurana RN, Wieland MR, Boldrey EE, et al. Vitelliform retinopathy in metastatic cutaneous melanoma with choroidal involvement. Arch Ophthalmol. 2011; 129:1498–1499. [PubMed: 22084223]
26. Koreen L, He SX, Johnson MW, et al. Anti-retinal pigment epithelium antibodies in acute exudative polymorphous vitelliform maculopathy: a new hypothesis about disease pathogenesis. Arch Ophthalmol. 2011; 129:23–29. [PubMed: 21220625]

Author Manuscript Author Manuscript Author Manuscript Author Manuscript

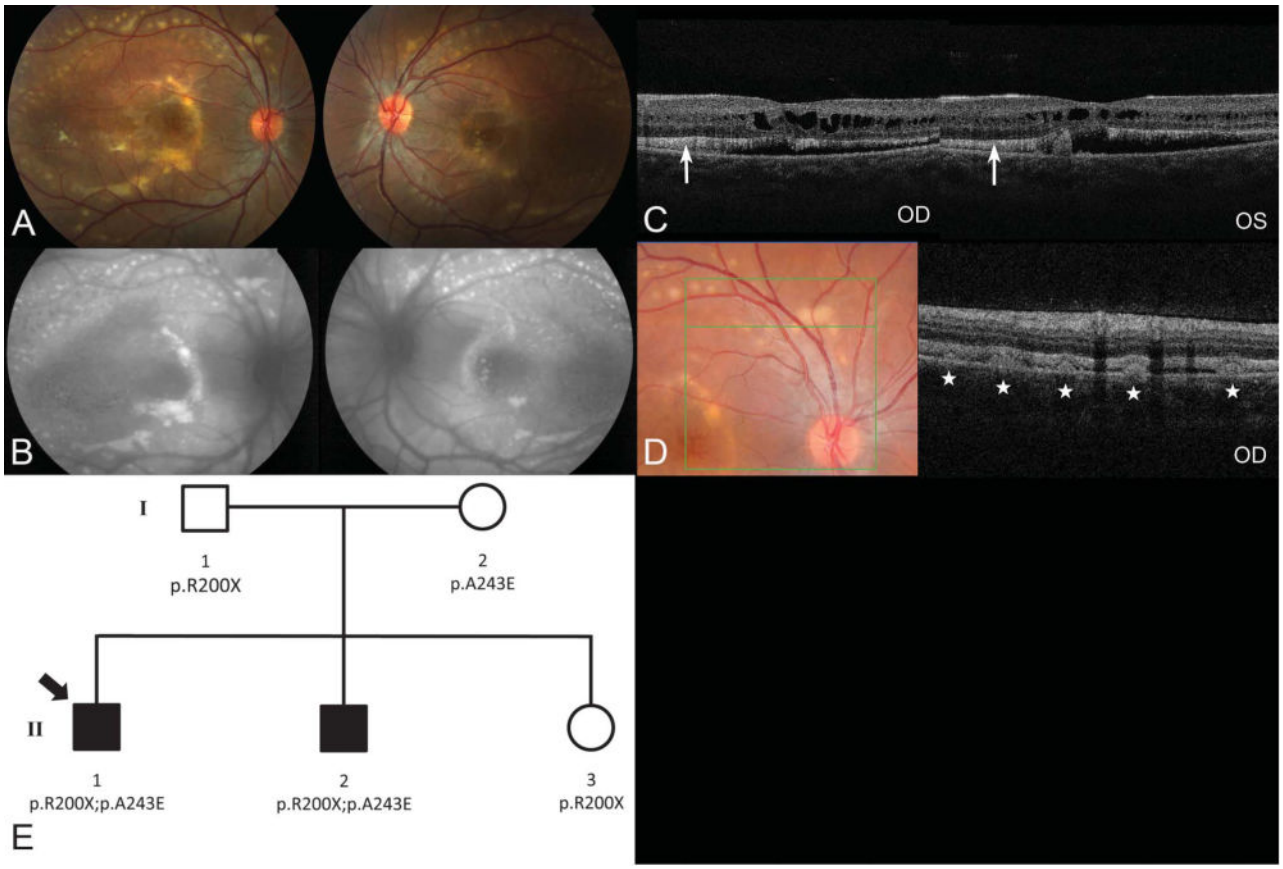

Fig. 1.

Family 1, Patient 1. A 11-year-old otherwise healthy white boy presented with a 6-month history of reduced vision and central scotoma. **A.** Color fundus photographs demonstrate bilateral, multifocal subretinal yellowish deposits within the posterior pole extending up to the equator. **B.** There is intense hyperautofluorescence (Topcon TRC-50DX retinal camera; Topcon America, Paramus, NJ) of the yellowish deposits and moderate hyperautofluorescence in the areas of subretinal fluid. **C.** Spectral domain optical coherence tomography (Topcon 3D-OCT 2000) horizontal scans through the maculae reveal cystoid macular changes and shallow serous macular detachments in both eyes. There is thickening and hyperreflectivity at the inner segment/outer segment photoreceptor junction ("Band 2," arrows). **D.** Spectral domain optical coherence tomography horizontal scan through the superior vascular aracade, 3 months after presentation colocalizes the vitelliform material to the subretinal space. The material appears to be emanating from the RPE (stars). **E.** Genetic screening of the family members confirmed the segregation of the two *BEST1* mutations with the disease.

Author Manuscript Author Manuscript Author Manuscript Author Manuscript

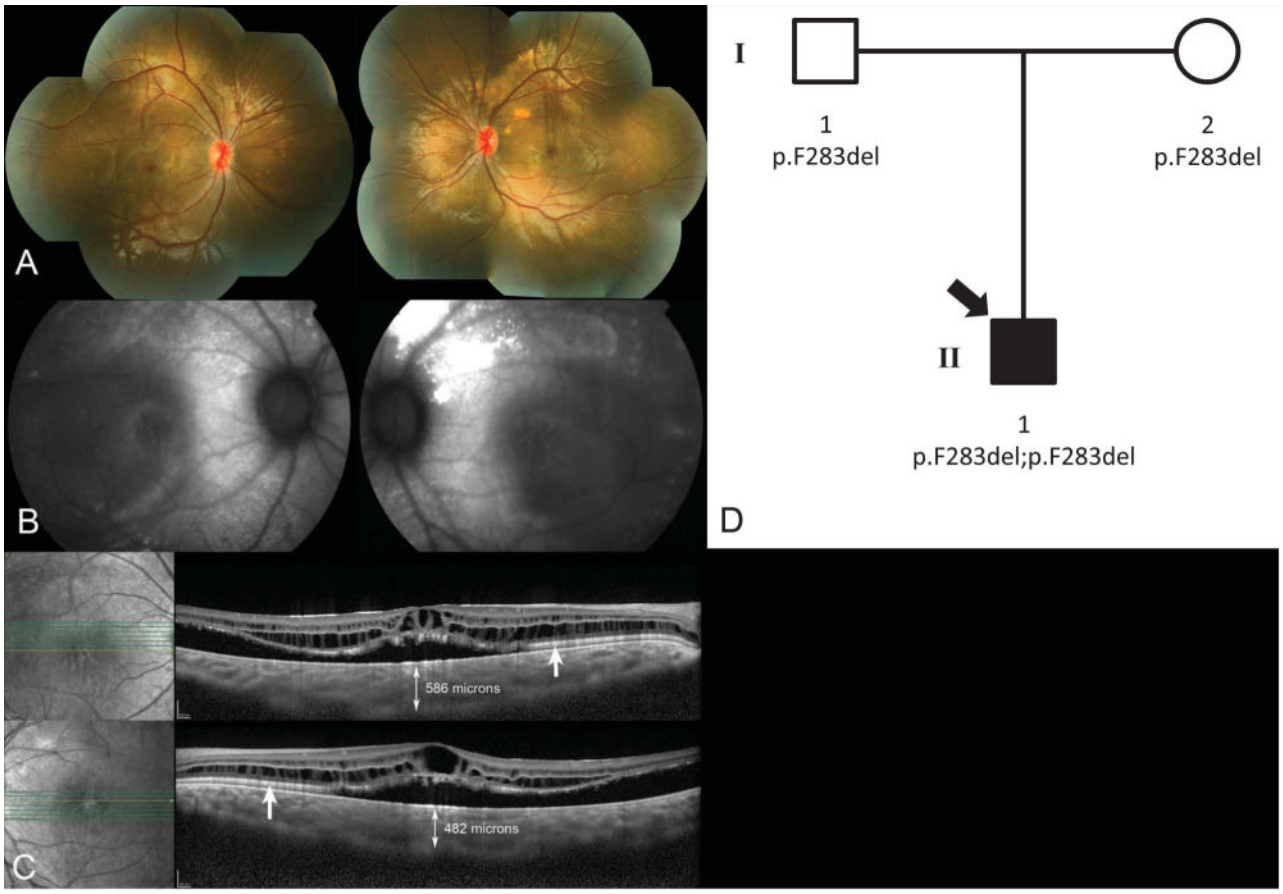

Fig. 2.

Family 2, Patient 3. A 6-year-old asymptomatic, U.S.–born African boy was noted to have poor vision by his schoolteacher. **A.** Color montage fundus photographs. In the right eye, there is subtle vitelliform material nasal to the optic disk. In the left eye, multifocal, curvilinear subretinal yellowish deposits are seen along the superotemporal arcade. **B.** Fundus autofluorescence imaging (Topcon TRC-50DX retinal camera; Topcon America) demontrates hyperautofluorescence of the vitelliform material in the left eye. **C.** Enhanced depth imaging spectral domain optical coherence tomography (Heidelberg Spectralis HRA +OCT; Heidelberg Engineering Inc, Heidelberg, Germany) demonstrates bilateral shallow subretinal fluid involving the maculae, a cystoid maculopathy, and subfoveal choroidal thicknesses of 586 μm in the right eye and 482 μm in the left eye. There is thickening and hyperreflectivity at the inner segment/outer segment photoreceptor junction (“Band 2,” arrows). **D.** The consanguineous parents had normal retinal examinations, 20/20 vision in both eyes and normal quantitative fundus autofluorescence imaging. Two older brothers and one sister, who were not available for genetic screening, were visually asymptomatic with 20/20 vision in both eyes.

Author Manuscript Author Manuscript Author Manuscript Author Manuscript

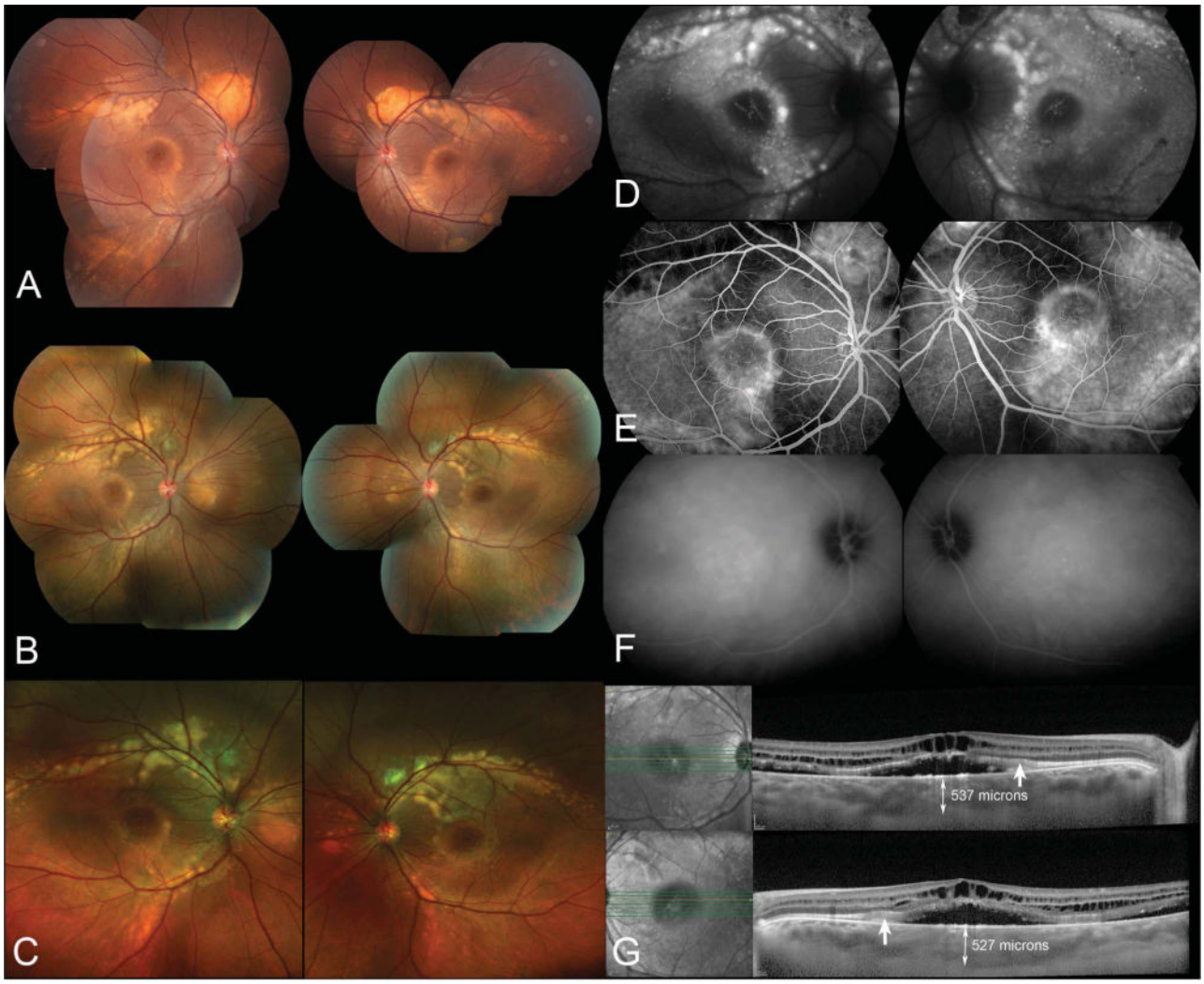

Fig. 3.

Family 3, Patient 4. A 12-year-old otherwise healthy, emmetropic Puerto Rico-born U.S. boy was noted to have reduced vision on routine eye examination. **A.** Montage color fundus photographs at initial presentation. There are bilateral, confluent curvilinear subretinal yellowish vitelliform deposits superior to the optic disks, along the temporal vascular arcades and encircling the maculae. **B** and **C**. Color fundus photographs 3 years later. The vitelliform material has become more multifocal and dispersed to involve the nasal retinae. Visual acuities remained stable at 20/60 in the right eye and 20/70 in the left eye. **D.** Fundus autofluorescence imaging (Topcon TRC-50DX retinal camera; Topcon America) demonstrates hyperautofluorescence of the vitelliform material. **E.** On fluorescein angiography (Topcon TRC-50DX; 61 seconds for the right eye, 92 seconds for the left eye), there is widespread diffuse hyperfluorescence consistent with pooling in the subretinal space and staining of the subretinal yellowish deposits. **F.** Indocyanine green angiography (Topcon TRC-50DX; 11 minutes 43 seconds for the right eye, 12 minutes 7 seconds for the left eye) demonstrates bilateral midphase hyperfluorescence at the maculae. **G.** On spectral domain optical coherence tomography (Spectral OCT/SLO; OPKO Instrumentation, Miami, FL),

there are bilateral, multifocal serous retinal detachments involving the maculae and cystoid changes in the macula. There is thickening and hyperreflectivity at the inner segment/outer segment photoreceptor junction (“Band 2”, arrows). Subfoveal choroidal thickness measured 537 μm in the right eye and 527 μm in the left eye with enhanced depth imaging.

Author Manuscript Author Manuscript Author Manuscript Author Manuscript

Author Manuscript Author Manuscript Author Manuscript Author Manuscript

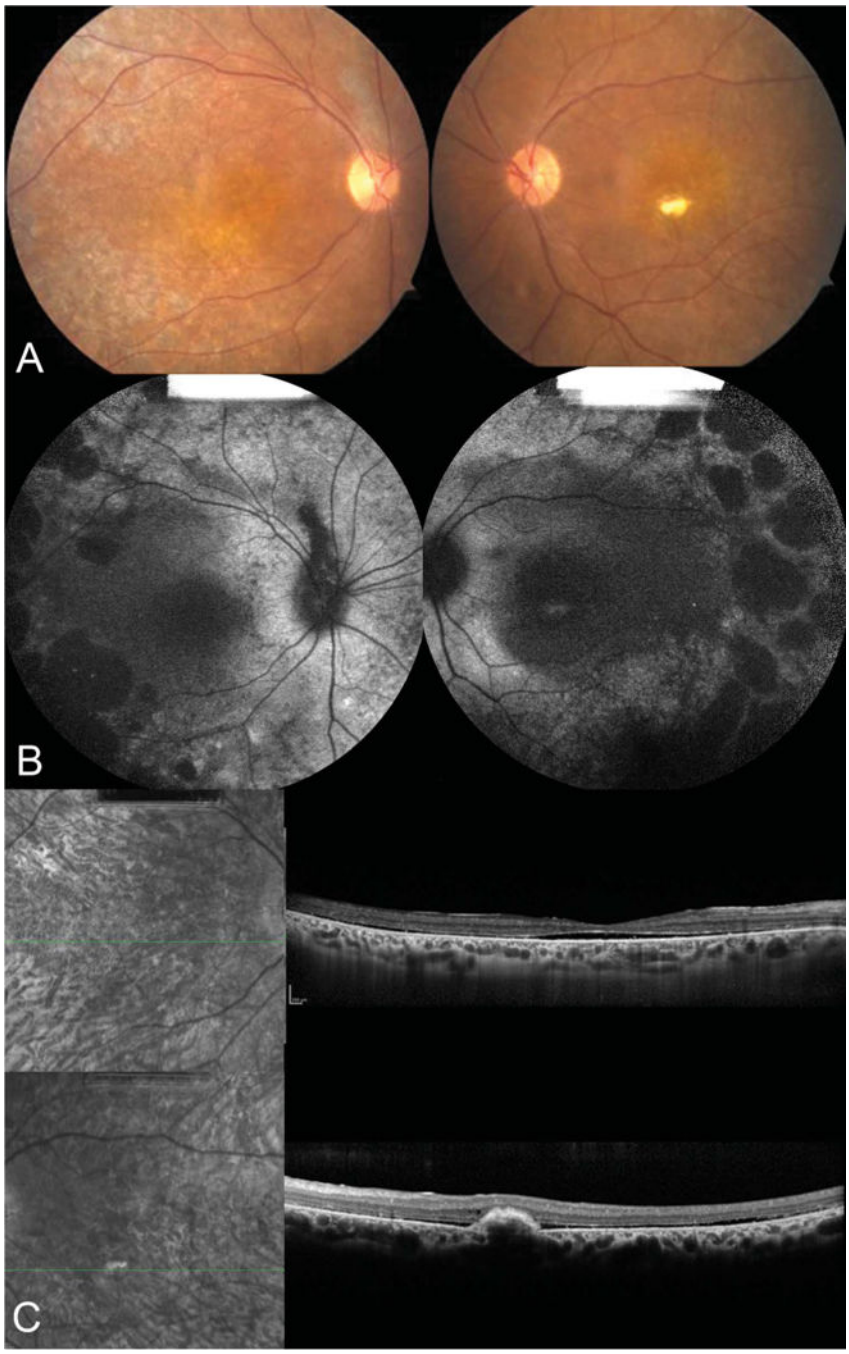

Fig. 4.

Family 4, Patient 5. A 42-year-old woman whose vision problems started at 5 years of age was recently noticing deteriorating central vision. She was the product of a first-cousin marriage. A. Color fundus photographs showing a white–yellow vitelliform lesion at the left fovea. There is RPE and retinal atrophy within the posterior poles. **B.** Fundus autofluorescence imaging shows bilateral discrete patches of hypoautofluorescence. The vitelliform lesion at the left fovea hyperautofluoresces. **C.** On spectral domain optical coherence tomography (Heidelberg Spectralis HRA+OCT; Heidelberg Engineering Inc),

shallow subretinal fluid is seen at both maculae but not cystoid maculopathy. The subretinal vitelliform deposit is seen in the left eye. Subfoveal choroidal thickness measured 370 μm in both eyes with enhanced depth imaging.

Author Manuscript Author Manuscript Author Manuscript Author Manuscript

Author Manuscript Author Manuscript Author Manuscript Author Manuscript

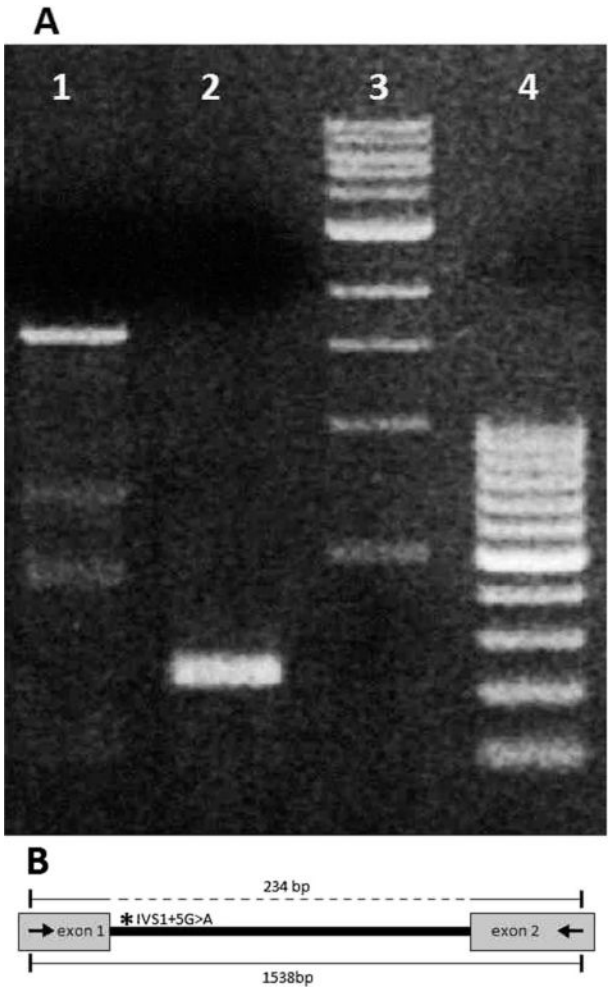

Fig. 5.

Analysis of splicing of the *BEST1* gene in Patient 5. Complementary DNA from Patient 5, harboring the IVS1+5G>A variant (**A**, Lane 1), and from a normal control individual (**A**, Lane 2) was amplified by primers located in Exons 1 and 2 of the *BEST1* gene. Amplification of the cDNA of a normal control produced the expected PCR fragment of 234bp (**A**, Lane 2). This 234bp PCR fragment corresponds to the correctly spliced fragment containing Exons 1 and 2, as shown in the dotted line above in (**B**). Amplification of the cDNA of the patient homozygous for the IVS1+5G>A variant did not yield the expected PCR product because the first intron (IVS1) was not spliced out, resulting in a large 1538bp PCR product which includes the entire IVS1 (**A**, Lane 1; **B**, line below). Lanes 3 and 4 show DNA size standards. cDNA, complementary DNA.

Author Manuscript Author Manuscript Author Manuscript Author Manuscript

Table 1

Clinical Features of Patients With ARB

Family	Patient (Age, Years/Gender)	Ethnicity	Follow-up Duration	Snellen Best-Corrected Visual Acuity on Presentation	Snellen Best-Corrected Visual Acuity at Last Visit	Refraction, Diopters	Anterior Chamber Angle	Fundus Appearance
1	1 (11/M)	White	4 months	20/22 OU	20/50	−2.50 D OD, −2.75 D OS	Open	Bilateral multifocal vitelliform deposits
1	2 (7/M)	White	0 months	20/25 OU	20/25 OU	Unknown	Open	Bilateral multifocal vitelliform deposits
2	3 (6/M)	African	3 years	20/80 OD, 20/100 OS	20/80 OU	+4.00 OD, +4.25 D OS	Open	Bilateral multifocal vitelliform deposits
3	4 (12/M)	Latino	3 years	20/90 OU	20/60 OD, 20/70 OS	Emmetropic axial lengths: 21.6 mm OD, 21.3 mm OS	Open	Bilateral multifocal vitelliform deposits
4	5 (42/F)	Caucasian	3 months	20/150 OU	20/150 OU	+10.00D OD, +10.00D OS	Shallow	Left foveal vitelliform deposit

D, diopters; OD, right eye; OS, left eye; OU, both eyes.

Retina. Author manuscript; available in PMC 2015 May 09.

Author Manuscript Author Manuscript Author Manuscript Author Manuscript

Table 2

Investigations of Patients With ARB

			OCT				
Family	**Patient**	**FAF**	**CME**	**SRF**	**Subfoveal Choroidal Thickness**	**ERG**	**EOG**
1	1	Hyperautofluorescent vitelliform material	Y	Y	Unknown	Not performed*	Arden index: 2.1 OD, 2.6 OS
1	2	Hyperautofluorescent vitelliform material	Y	Y	Unknown	Not performed†	Not performed
2	3	Hyperautofluorescent vitelliform material	Y	Y	596 μm OD, 482 μm OS	Extinguished scotopic and photopic ffERG	Arden index: 1.0 OU
3	4	Hyperautofluorescent vitelliform material	Y	Y	537 μm OD, 527 μm OS	Diminished scotopic and photopic ffERG	Failed recording‡
4	5	Bilateral discrete patches of hypoautofluorescence, with hyperautofluorescence at the left macula	N	Y	370mm OD, 370mm OS	Diminished scotopic and photopic ffERG	Arden index: 1.55 OD, 1.67 OS

*ERG not performed on the day of EOG. The patient will not have separate ERG done.

†ERG and EOG not performed because of incapacity of the patient to come in to have the International Society for Clinical Electrophysiology of Vision recordings performed.

‡EOG recordings were performed but failed. The patient is not capable of returning for new EOG testing.

EOG, electrooculography; ERG, electroretinography; FAF, fundus autofluorescence; OCT, optical coherence tomography; OD, right eye; OS, left eye; OU, both eyes; CME, cystoid macular edema; SRF, subretinal fluid.

Retina. Author manuscript; available in PMC 2015 May 09.

Author Manuscript Author Manuscript Author Manuscript Author Manuscript

Table 3

In Silico Analysis of the Five *BEST1* Mutations Found in Four Patients/Families

Family/Patient (Remark)	cDNA Position	Protein Position	Conservation	SIFT	PolyPhen-2	Mutation Taster	Splicing
1/1 and 2 (Compound heterozygous mutations)	**c.728C>A**	**p.Ala243Glu**	Highly conserved nucleotide (phyloP: 5.77); highly conserved amino acid (up to *C. elegans*)	Deleterious (score: 0.01, median: 3.07)	Probably damaging, score: 1.000 (sensitivity: 0.00; specificity: 1.00)	Disease-causing (*P*: 1.0)	N/A
	c.598C>T	p.Arg200*	Moderately conserved nucleotide (phyloP: 2.95); moderately conserved amino acid (up to Tetraodon)	N/A	N/A	N/A	N/A
2/3 (Homozygous mutation)	**c.847_849del**	**p.Phe283del**	Highly conserved amino acid (up to *C. elegans*)	N/A	N/A	N/A	MaxEnt: 0.0%, NNSPLICE: 0.0%
3/4 (Homozygous mutation)	c.821C>G	p.Pro274Arg	Highly conserved nucleotide (phyloP: 5.61); highly conserved amino acid (up to *C. elegans*)	Deleterious (score: 0.00, median: 3.07)	Probably damaging, score: 1.000 (sensitivity: 0.00; specificity: 1.00)	Disease-causing (*P*: 1.0)	N/A
4/5 (Homozygous mutation)	**IVS1+5G>A**	N/A	Moderately conserved nucleotide (phyloP: 1.42)	N/A	N/A	N/A	MaxEnt: −100.0%, NNSPLICE: −97.7%

Mutations in bold are novel mutations.

cDNA, complementary DNA; SIFT, sorting intolerant from tolerant; N/A, not applicable.